

Eliminating Delocalization Error through Localized Orbital Scaling Correction with Orbital Relaxation from Linear Response

Yichen Fan,¹ Jincheng Yu,^{1, a)} Jiayi Du,¹ and Weitao Yang¹

Department of Chemistry, Duke University, Durham, NC 27708^{b)}

(*Electronic mail: weitao.yang@duke.edu)

(Dated: February 12, 2026)

Despite the great success Kohn-Sham density functional theory (KS-DFT) has achieved, the delocalization error remains a major challenge for commonly used density functional approximations (DFAs), resulting in systematic errors in ionization energies, electron affinities, band structures, and charge distributions. A recently developed localized orbital scaling correction (LOSC) method, namely linear response LOSC (lrLOSC), addresses these challenges by incorporating a functional correction that includes the screening effect and orbital localization within the LOSC framework. The method has been shown to provide accurate descriptions of bulk systems and core-level binding energies in small molecular systems. In this work, we extend the applicability of lrLOSC to a broader range of molecular systems, spanning various sizes, with a focus on the corrections to valence orbital energies and total energies. To enable the calculation of large chemical systems, we developed an efficient implementation of lrLOSC with computational costs comparable to standard KS-DFT calculations. Numerical results show that, while screening provides modest improvements for small molecules, it becomes critical for achieving high accuracy in larger molecules, from linear to three-dimensional systems. With the screening effect well captured in a unified way, lrLOSC provides accurate descriptions for a wide range of chemical systems, including organic molecular systems of varying sizes and transition-metal oxide complexes, establishing it as a powerful tool for enhancing the reliability of computational simulations of chemical systems.

Kohn-Sham density functional theory (KS-DFT)^{1–3} is highly regarded and widely used to describe the electronic structures of molecules and bulk systems in chemistry, physics, and materials science at a feasible computational cost. Driven by the need for accurate predictions from DFT-based theoretical simulations, the development of density functional approximations (DFAs) has become a vibrant research area in quantum chemistry. Over the past few decades, conventional DFAs, including local density approximations (LDAs)⁴, generalized gradient approximations (GGAs)^{5–7}, meta-GGAs^{8–12}, hybrid functionals^{5,6,13} and range-separated hybrid functionals^{14–17} have achieved significant success.

Despite their great success, conventional DFAs suffer from major drawbacks: inaccurate valence orbital energies^{18–21}, underestimated reaction barriers²², and inaccurate charge distribution descriptions^{23,24}. . . These shortcomings originate from a systematic error known as the delocalization error^{25,26} (DE), which exhibits a size-dependent behavior. For small chemical systems with limited physical extent, DE manifests as a violation of the Perdew-Parr-Levy-Balduz (PPLB) condition^{27,28}, which states that the exact total energy $E(N)$, as a function of the number of electrons, should be piecewise linear between consecutive integer values of N . Energies from conventional DFAs are generally reliable at integer points, but display a convex deviation from the PPLB condition^{27,28} at fractional electron numbers. As the size of the system increases, this convex deviation decreases and disappears at the bulk limit.²⁵ However, at the large

system and bulk limit, the DE manifests differently: conventional DFAs produce quantitatively incorrect total energies for charged systems at integer electron numbers²⁵. To eliminate the systematic DE, many methods have been developed, including range-separated hybrid functionals^{29,30}, dielectric-dependent hybrid functionals³¹, self-interaction error corrected functionals^{32,33}, DFT+U approaches^{34,35}, and Koopmans-compliant functionals^{36,37}.

In addition to the aforementioned methods, a series of scaling correction (SC) methods^{23,38–43} have been developed. Extensive numerical studies have shown that SC methods effectively eliminate DE and provide accurate numerical descriptions for numerous critical problems, such as the photoemission spectroscopy^{23,42,44,45}, photoexcitation energies^{44,46–48}, fundamental gaps^{23,38,44}, and polarizability^{39,49}.

Building upon these successes, a novel SC method, namely linear-response localized orbital scaling correction (lrLOSC), has recently been developed. This method has demonstrated remarkable accuracy, as evidenced by its successful applications to bulk materials⁵⁰ and core-level binding energies in small molecular systems⁵¹. The high accuracy of lrLOSC stems from its two critical components: orbital localization and orbital relaxation, the latter of which is effectively captured with the linear response theory.

In this work, we extend lrLOSC's applicability to molecular systems of all sizes, highlighting its capability to provide accurate corrections to both total energies and valence orbital energies. Specifically, we aim to evaluate the roles of orbital localization and orbital relaxation (or the screening effect) in molecular systems. We begin by introducing the theoretical framework of lrLOSC, outlining its key components and implementation details. We then present numerical results from our calculations, demonstrating the effectiveness and efficiency of lrLOSC in its current implementation.

^{a)}Present address: Department of Chemistry and Biochemistry, University of Maryland, College Park, MD 20742

^{b)}Department of Physics, Duke University, Durham, NC 27708

In lrLOSC, the correction to the total energy, ΔE_{lrLOSC} , defined as the difference between the total energy from lrLOSC, E_{lrLOSC} , and the total energy from a DFA, E_{DFA} , is given by

$$\Delta E_{\text{lrLOSC}} \equiv E_{\text{lrLOSC}} - E_{\text{DFA}} = \frac{1}{2} \sum_{\sigma} \sum_{pq} \kappa_{pq}^{\sigma} \lambda_{pq}^{\sigma} (\delta_{pq} - \lambda_{pq}^{\sigma}), \quad (1)$$

where κ^{σ} is the curvature matrix for spin σ , and λ^{σ} is the localized orbital (LO) occupation matrix, $\lambda_{pq}^{\sigma} = \langle \phi_{p\sigma} | \hat{\rho} | \phi_{q\sigma} \rangle$. In lrLOSC, the LOs $\{\phi_{p\sigma}\}$ are also called orbitalets, and they are localized in both the physical space and the energy space. Based on Eq. (1), to obtain the energy correction from lrLOSC, the two main tasks are a) constructing the orbitalets and calculate the LO occupation matrix λ^{σ} and b) constructing the curvature matrix κ^{σ} . We will describe how to complete the two tasks in lrLOSC respectively.

The localization procedure employed in lrLOSC is from the second version of LOSC (LOSC2)⁴¹. Orbitalets are constructed through a unitary transformation of the canonical molecular orbitals (CMOs) $|\psi_n^{\sigma}\rangle$ in both the occupied and virtual subspaces for each spin channel σ

$$|\phi_p^{\sigma}\rangle = \sum_n U_{pn}^{\sigma} |\psi_n^{\sigma}\rangle, \quad (2)$$

where the linear coefficients U_{pn}^{σ} are determined by minimizing the cost function F^{σ} .

$$F^{\sigma} = (1 - \gamma) \sum_p \left[\langle \phi_p^{\sigma} | r^2 | \phi_p^{\sigma} \rangle - \langle \phi_p^{\sigma} | r | \phi_p^{\sigma} \rangle^2 \right] + \gamma C \sum_p \left[\langle \phi_p^{\sigma} | \hat{h}^2 | \phi_p^{\sigma} \rangle - \langle \phi_p^{\sigma} | \hat{h} | \phi_p^{\sigma} \rangle^2 \right], \quad (3)$$

which represents a weighted sum of the physical-space cost function $\sum_p [\langle \phi_p^{\sigma} | r^2 | \phi_p^{\sigma} \rangle - (\langle \phi_p^{\sigma} | r | \phi_p^{\sigma} \rangle)^2]$ and the energy-space cost function $\sum_p [\langle \phi_p^{\sigma} | \hat{h}^2 | \phi_p^{\sigma} \rangle - (\langle \phi_p^{\sigma} | \hat{h} | \phi_p^{\sigma} \rangle)^2]$, where \hat{h} is the (generalized) KS one-electron Hamiltonian. In Eq. (3), γ is the weight of the energy-space cost function, restricted to $0 \leq \gamma \leq 1$, and C is equal to $1 \text{ \AA}^2 \text{ eV}^2$. Note that a similar cost function was developed by Gygi and others^{52–54} for bulk systems, but restricted to the occupied states (valence band) alone. In contrast, for both molecular and bulk systems, our localization procedure is applied to all states, including occupied and virtual, or equivalently the valence and conduction bands. The resulting LOs correspond to molecular orbitalets⁴¹ in finite systems and to dually localized Wannier functions in periodic materials⁵⁵.

The localization in Eq. (3) can be understood based on its limits. When $\gamma = 1$, F^{σ} encompasses solely the energy localization, making the orbitalets equivalent to CMOs. When $\gamma = 0$, all energy information is sacrificed to achieve the maximum localization in the physical space. At this limit, F^{σ} closely resembles the cost function of the Foster-Boys localization⁵⁶; yet a major distinction arises: the linear combination in Eq. (2) extends to both occupied and virtual orbitals. This inclusion allows the presence of fractionally occupied orbitals, further enabling total energy corrections for physical

systems with an integral number of electrons⁴¹. In practical computations for lrLOSC, the parameter $\gamma = 0.477(\text{eV}^2 / \text{\AA}^2)$ is consistently applied across different systems^{23,41}. This value leads to optimal orbitalets with dynamic behavior, meaning that they adapt to the system's geometry and can be just canonical orbitals or space localized orbitals, depending on the one-electron energy spectrum at the specific geometry.

In small systems with limited physical extent, like a water molecule at its equilibrium geometry, there is often a notable energy gap between the occupied orbitals and the virtual orbitals. This significant energy gap results in a high cost for the localization in the energy space when one attempts to mix occupied and virtual orbitals. Therefore, the derived orbitalets closely resemble canonical orbitals with very little mixing between occupied and virtual orbitals. On the other hand, as the system size increases or the chemical bonds are stretched, the energy gap between occupied and virtual orbitals decreases, enhancing the significance of spatial localization. This leads to spatially localized orbitals that can exhibit considerable fractional occupations within λ_{pq}^{σ} . Therefore, in smaller systems, the dynamic localization of orbitalets produces diagonal and integer values for λ_{pp}^{σ} , whereas for larger systems, fractional λ_{pp}^{σ} values are commonly observed^{23,41}. In addition to serving as intermediate orbitals for computing lrLOSC corrections, orbitalets can also qualitatively reveal the chemically reactive regions of various systems^{57,58}.

Now we introduce the second component of lrLOSC, namely the curvature matrix. In lrLOSC, the curvature matrix κ^{σ} employed in Eq. (1) is designed to include the screening effect or orbital relaxation. In the initial version of LOSC^{23,41}, the frozen orbital approximation was adopted as the global scaling correction (GSC)³⁸, providing accurate predictions for both small and large molecules. However, this approximation significantly overestimates the band gaps for bulk systems⁵⁹, making it unsuitable as a universal approach. Incorporating orbital relaxation has shown improvements in orbital energies^{40,42}. A clear and straightforward formulation of orbital relaxation in κ_{pq} was initially presented for frontier orbitals during the earlier development⁶⁰ of GSC, and was later extended to all canonical orbitals and to include cross terms by Mei, Chen, and Yang⁴². The results of the Koopmans-compliant functional in orbital energies further underscores the importance of orbital relaxation.³⁷

The expression of the curvature matrix in lrLOSC can be derived from several approaches, including the coupled perturbed equations, the combination of the Maxwell relation and linear response, and using the density matrix as the direct variable, as documented in the supporting information (SI) of Ref. 42. The form of the curvature matrix is

$$\kappa_{pq}^{\sigma} = K_{pp\sigma,qq\sigma} - \sum_{iat,jbv} (K_{pp\sigma,iat} + K_{pp\sigma,ait}) M_{iat,jbv}^{-1} K_{jbv,qq\sigma}, \quad (4)$$

and

$$M_{iat,jbv} = (\varepsilon_{at} - \varepsilon_{it}) \delta_{ij} \delta_{ab} \delta_{tv} + (K_{iat,jbv} + K_{iat,bjv}), \quad (5)$$

where i, j are indices for occupied CMOs, a, b are indices for virtual CMOs, p, q are indices for orbitalets, and σ, τ, v

are spin indices. The matrix $M_{ia\sigma,jb\tau}$ was derived by Yang *et al.*⁶⁰. In Eq. (5), the Hartree-exchange-correlation kernel matrix $K_{pq\tau,rsv}$ is

$$K_{pq\tau,rsv} = \int d\mathbf{r}_1 d\mathbf{r}_2 d\mathbf{r}_3 d\mathbf{r}_4 \varphi_{p\tau}(\mathbf{r}_1) \varphi_{q\tau}^*(\mathbf{r}_2) \times K^{\sigma,\tau}(\mathbf{r}_1, \mathbf{r}_2; \mathbf{r}_3, \mathbf{r}_4) \varphi_{rV}^*(\mathbf{r}_3) \varphi_{sV}(\mathbf{r}_4), \quad (6)$$

where

$$K^{\sigma,\tau}(\mathbf{r}_1, \mathbf{r}_2; \mathbf{r}_3, \mathbf{r}_4) = \frac{\delta(\mathbf{r}_1, \mathbf{r}_2) \delta(\mathbf{r}_3, \mathbf{r}_4)}{|\mathbf{r}_1 - \mathbf{r}_3|} + \frac{\delta^2 E_{xc}}{\delta \rho_s^\sigma(\mathbf{r}_2, \mathbf{r}_1) \delta \rho_s^\tau(\mathbf{r}_3, \mathbf{r}_4)}. \quad (7)$$

E_{xc} is the exchange-correlation (xc) energy evaluated from DFA.

With both the LO occupation matrix and the curvature matrix constructed, we now have the expression for the orbital energies from lrLOSC

$$\begin{aligned} \varepsilon_{i\sigma}^{\text{LOSC}} &= \frac{\partial E_{\text{LOSC}}}{\partial n_i^\sigma} \\ &= \varepsilon_{i\sigma}^{\text{DFA}} + \sum_p \left[\left(\frac{1}{2} - \lambda_{pp}^\sigma \right) \kappa_{pp}^\sigma |U_{pi}^\sigma|^2 - \sum_{q \neq p} \kappa_{pq}^\sigma \lambda_{pq}^\sigma U_{pi}^\sigma U_{qi}^{\sigma*} \right], \end{aligned} \quad (8)$$

where U is the unitary matrix in Eq. (2). Note that the γ is the only parameter in the cost function, which can be used to directly correct the DE in any DFA without requiring additional tuning.

While the inclusion of screening effects significantly enhances the accuracy of lrLOSC, it also brings a considerable increase in computational cost compared to the original curvature matrix employed in LOSC^{23,41}. Specifically, constructing the curvature matrix κ requires inverting the matrix \mathbf{M} in Eq. (5), which demands extensive computational resources, both in terms of time and memory. The \mathbf{M} matrix has a dimension of $N_{occ}N_{vir} \times N_{occ}N_{vir}$, where N_{occ} designates the number of occupied orbitals, and N_{vir} denotes the number of virtual states. Calculating the inverse of \mathbf{M} directly makes lrLOSC an $\mathcal{O}(N^6)$ algorithm, with N being the number of electrons. The high computational cost will restrict the application of lrLOSC to small and medium-sized systems.

To broaden the applicability of lrLOSC, in this study, we introduce an alternative way to compute κ , which leverages the algebraic structure of the matrix \mathbf{M} and utilizes a Resolution-of-Identity^{61,62} approximation (RI-V), thereby reducing the time complexity of lrLOSC to $\mathcal{O}(N^3)$ alongside a straightforward $\mathcal{O}(N^4)$ step.

The conventional RI-V scheme⁶² decomposes the four-center electron repulsion integrals into products of two- and three-center integrals using the atomic-centered auxiliary basis functions $\{f_P(\mathbf{r})\}$, such that:

$$(ia|jb) = \sum_{PQ} C_{ia}^P V_{PQ}^{-1} C_{jb}^Q, \quad (9)$$

where V_{PQ}^{-1} is the inversion of the two-center Hartree integral

$$V_{PQ} = \int d\mathbf{r} d\mathbf{r}' f_P(\mathbf{r}) \frac{1}{|\mathbf{r} - \mathbf{r}'|} f_Q(\mathbf{r}'), \quad (10)$$

and C_{ia}^P are the expansion coefficients which are chosen to be

$$C_{ia}^Q = \sum_P (ia|P) V_{PQ}^{-1}. \quad (11)$$

To accommodate the xc contribution in \mathbf{K} , we extend the conventional RI-V scheme in lrLOSC as follows:

$$K_{ia\tau,jbv} = \iint d\mathbf{r} d\mathbf{r}' \frac{\varphi_{i\tau}(\mathbf{r}) \varphi_{a\tau}^*(\mathbf{r}) \varphi_{jv}^*(\mathbf{r}') \varphi_{bv}(\mathbf{r}')}{|\mathbf{r} - \mathbf{r}'|} + \varphi_{i\tau}(\mathbf{r}) \varphi_{a\tau}^*(\mathbf{r}) f_{xc}^{\tau V} \varphi_{jv}^*(\mathbf{r}') \varphi_{bv}(\mathbf{r}'), \quad (12)$$

$$\approx \sum_{PQRS} C_{ia\tau}^P V_{PQ}^{-1} (V_{QR} + f_{QR}^{xc}) V_{RS}^{-1} C_{jbv}^S, \quad (13)$$

and f_{xc} is the second functional derivative used in time dependent-DFT.

This RI-like approximation provides a compact, lower-rank representation for \mathbf{K} , allowing the matrix \mathbf{M} to be efficiently restructured as:

$$\mathbf{M} = \mathbf{A} + \mathbf{X} \cdot \mathbf{Y}^T, \quad (14)$$

where

$$A_{ia\tau,jbv} = (\varepsilon_{a\tau} - \varepsilon_{i\tau}) \delta_{ij} \delta_{ab} \delta_{\tau v}, \quad (15)$$

$$X_{ia\tau,Q} = \sum_P C_{ia\tau}^P V_{PQ}^{-1}, \quad (16)$$

$$Y_{Q,jbv} = \sum_{RS} (V_{QR} + f_{QR}^{xc}) V_{RS}^{-1} C_{jbv}^S. \quad (17)$$

By leveraging the decomposition in Eq. (14), we apply the Sherman-Morrison-Woodbury (SMW) formula⁶³, which enables the efficient inversion of matrix \mathbf{M} as:

$$\mathbf{M}^{-1} = \mathbf{A}^{-1} - \mathbf{A}^{-1} \mathbf{X} (\mathbf{I} + \mathbf{Y}^T \mathbf{A}^{-1} \mathbf{X})^{-1} \mathbf{Y}^T \mathbf{A}^{-1}. \quad (18)$$

Here, \mathbf{A} is diagonal, and \mathbf{X} and \mathbf{Y} are lower-rank three-center matrices with dimensions $(N_{occ}N_{vir}) \times N_{aux}$, where N_{aux} represents the number of auxiliary functions in $\{f_P\}$, and N_{aux} is significantly smaller than $N_{occ}N_{vir}$. This setup provides an efficient compromise between computational cost and memory usage. As a result, evaluating the lrLOSC curvature becomes practical for larger molecular systems. Further details on this RI implementation and the associated time-scaling analysis can be found in the first section of the SI. This resolution of the identity approximation is able to reduce the computational cost to a $N_{aux} \times N_{aux}$ matrix inversion plus a straightforward summation in the $(N_{occ} \times N_{vir})^2$ space.

With the new implementation, we test the capability of lrLOSC for providing accurate corrections to the valence orbital energies and the total energies of molecular systems of different sizes. The frontier orbital energies from lrLOSC offer valuable insights into the chemical potential, $\left(\frac{\partial E}{\partial N}\right)_v$, which describes the energy change associated with the electron addition and removal processes. Therefore, frontier orbital energies are directly connected to the ionization potential (IP) and electron affinity (EA).^{44,64,65} In this study, we compare the valence orbital energies from lrLOSC with those

obtained from the global scaling correction with the analytical and exact second-order corrections (denoted as GSC2)⁴², which incorporates the screening effect based on CMOs, and LOSC2⁴¹, which employs orbitalets but captures no orbital relaxation. Through these comparisons, we show the importance of the two theoretical components of IrLOSC: orbital localization and the electron screening effect. We also compare the results from IrLOSC with those from Δ -SCF, which evaluates the first IP and EA through the total energy difference between the neutral species and the $(N \pm 1)$ -electron systems.

To gain a comprehensive picture of the performance of IrLOSC, considering that DE exhibits different behaviors as the molecular size increases, IrLOSC was tested on molecules of varying sizes^{66–68} as well as in transition metal monoxide molecules. The complete test set is divided into four categories: small molecules (with a maximum of six atoms), large non-linear molecules (containing more than eight atoms, excluding polymers), polyacetylene ($\text{H}(\text{HC}=\text{CH})_n\text{H}$, $n \in [1, 10]$), and transition metal oxides. Please refer to the SI for more details on the systems.

In Figure 1, the mean absolute errors (MAEs) for IP are plotted across different methods. All calculations were performed based on the PBE functional⁷. All IrLOSC, LOSC2, and GSC2 calculations are performed as a post-SCF calculation. In Figure 2, a similar comparison is shown for the EA. For the transition metal monoxides, the $(N \pm 1)$ -electron system may be poorly defined, so the Δ SCF results are not provided. From Figure 1 and Figure 2, one can notice that IrLOSC consistently shows the lowest MAEs among the four methods studied and that the errors from IrLOSC remain stable as the system size increases. The high accuracy of IrLOSC for systems of all sizes is due to a) utilizing properly localized orbitalets and b) the well described screening effect. The role of orbital localization can be understood by comparing IrLOSC with GSC2. While the two methods achieve similar accuracy for small molecules, IrLOSC demonstrates significant improvement over GSC2 in the computation of large molecules and polymers, where a significant shift from LO to CO is anticipated. On the other hand, to understand the importance of describing the screening effect, we compare the results from IrLOSC with those from LOSC2. With the screening effect well captured, IrLOSC consistently achieves lower MAEs than LOSC2 across molecules of all sizes.

In this work, we also apply our IrLOSC method for the first time to transition metal systems, which constitute a broad class of strongly correlated materials. IrLOSC yields accurate IP and EA predictions for transition metal oxides and reduces the error of the original LOSC approach by about half, highlighting the crucial role of the screening effects incorporated through linear response theory in transition metal calculations. Nonetheless, because the systems considered here are diatomic molecules, orbital localization effects are minor, and the orbital energy predictions obtained from IrLOSC and GSC2 are therefore very similar.

Figure 3 illustrates the absolute deviation in IP from the reference values. For small systems, the discrepancy between the MAEs from IrLOSC and GSC2 is negligible. However, for systems containing more than 8 atoms, IrLOSC demonstrates

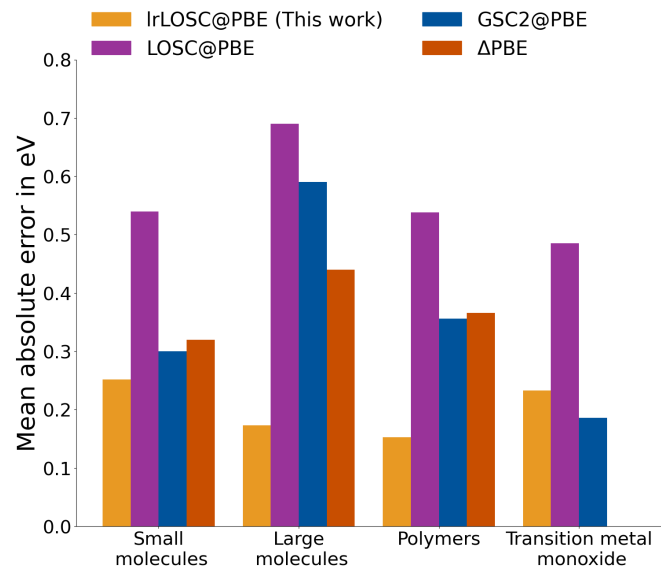


Figure 1. The MAEs of IPs, measured in eV, for gas-phase molecules of varying sizes obtained through different methods. The test set comprises 61 small molecules (containing no more than 8 atoms), 31 large non-linear molecules (with more than 8 atoms), poly-acetylene $\text{H}(\text{HC}=\text{CH})_n\text{H}$ (where n ranges from 1 to 10), and transition metal oxides from the fourth period. Note that, in general, orbital energies from the parent GGA functional deviate by more than 4 eV.

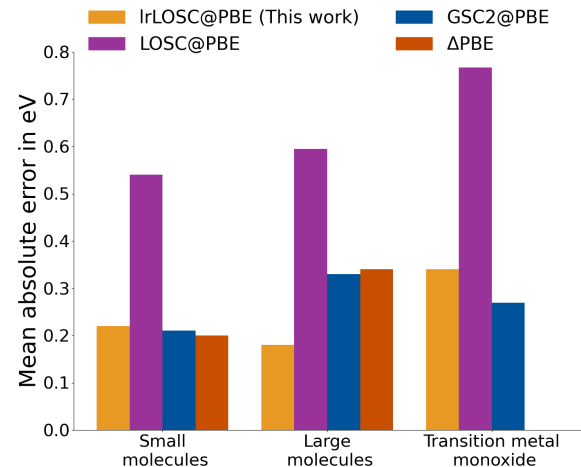


Figure 2. The MAEs of EAs, measured in eV, for gas-phase molecules of varying sizes obtained through different methods. The test set comprises 46 small molecules (containing no more than 8 atoms), 23 large non-linear molecules (with more than 8 atoms), and transition metal oxides from the fourth period. Note that, in general, orbital energies from the parent GGA functional deviate by nearly 3.5 eV.

superior performance over the GSC2 method.

IrLOSC shows promise in computing valence orbital energies. However, practical applications have exposed certain limitations of IrLOSC. Previous research indicates that in most conventional DFAs, it is primarily the quadratic com-

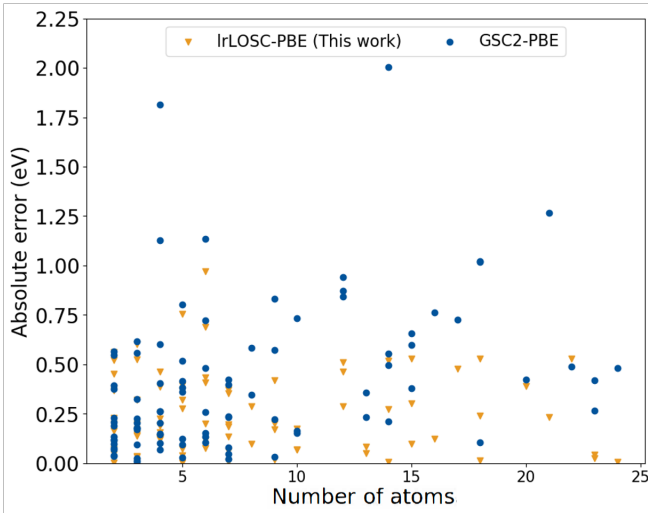


Figure 3. Error distribution of the first IP obtained from IrLOSC-PBE and GSC2-PBE for molecules with different sizes.

ponent that leads to deviations from the piece-wise linearity condition^{38,69}. Nevertheless, contributions from higher-order expansion can have a significant impact under some scenarios. An evidential example of these contributions from the higher-order expansion is the emergence of a negative-curvature region when a small fraction of an electron is added to certain integer systems.⁷⁰ This phenomenon is rare, but it does occur. The analytical expression of kappa in Eq. (4) can capture these unstable negative curvatures and lead to an unphysical energy correction.

To mitigate issues associated with negative curvature and enhance the robustness of IrLOSC for a wide range of systems, we developed an adjusted electron density to sidestep instability in the second derivative. For molecular orbitals exhibiting problematic elements in the curvature matrix, we introduced a slight increment in electron density when assessing the functional derivative of the xc functional. This addition assists the functional derivative in bypassing its unstable region while having minimal impact on other orbitals. Further details on convergence tests and implementations are available in the SI.

In addition to the valence orbital energies, accurately assessing the total energies is also crucial, particularly for larger systems where DE undermines the reliability of DFAs. Here, we demonstrate the effectiveness of IrLOSC in providing accurate total and orbital energies. Figure 4 shows the vertical IPs of tetracyanoethylene (TCNE) and benzonitrile calculated using three methods, compared with EOM-CCSD(T) benchmarks. IrLOSC provides positive energy corrections, particularly for ($N - 1$)-electron cationic systems, aligning the IPs more closely with EOM-CCSD(T) and highlighting the prominence of DE in charged systems. Table I reinforces this trend, showing systematic improvements in vertical IPs for 27 molecules, with a 0.14 eV reduction in MAE for IrLOSC-corrected Δ SCF compared to uncorrected methods. These results demonstrate IrLOSC as a robust method for addressing DE in both orbital and total energy calculations across diverse

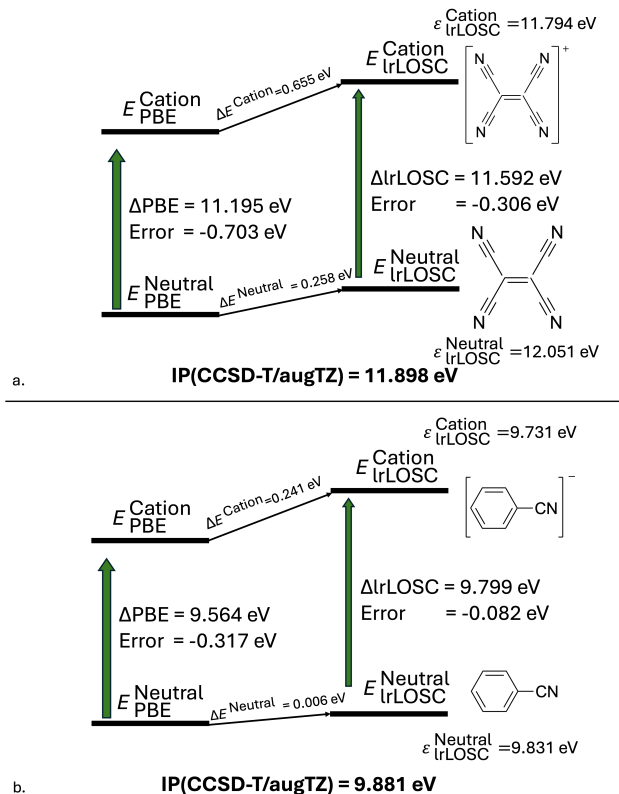


Figure 4. IrLOSC total energy correction (ΔE_{IrLOSC}) for (a) TCNE and its cation, and (b) benzonitrile and its cation. The vertical IPs are evaluated using three approaches: 1. The total energy difference between the cationic and neutral systems (indicated by green arrows), 2. The HOMO energy of the neutral system (bottom), and 3. The LUMO energy of the cationic system (top). The reference IP values are obtained from EOM-CCSD(T) calculations using the aug-cc-pVTZ basis set⁷¹. Errors relative to the EOM-CCSD(T) IP are reported beneath the total energy difference.

	$\epsilon_{\text{HOMO}}^{\text{Neutral}}$	ΔE_{PBE}	$\Delta E_{\text{IrLOSC-PBE}}$	ΔE_{Cation}	$\Delta E_{\text{Neutral}}$
MAE	0.16	0.44	0.30	0.22	0.03
MSE	-0.11	-0.43	-0.24	0.22	0.03

Table I. Comparison of vertical IPs for 27 large molecules derived from three methods. Both MAE and MSE are relative to EOM-CCSD(T)/aTZ computational results⁶⁷. In addition to the corrected total energy differences, the average IrLOSC total energy corrections to the neutral molecules and cations are reported in the last two columns labeled with $\Delta E_{\text{Neutral}}$ and ΔE_{Cation} .

molecular systems.

In summary, we present a non-empirical approach named lrLOSC that effectively eliminates the DE and provides estimates of the valence orbital spectrum with reliable accuracy across molecular systems of different sizes at low computational cost. The lrLOSC method addresses the DE by focusing on two principal aspects: orbital localization and the screening effect. Numerical findings suggest that lrLOSC offers accurate estimations of valence orbital energies and total energies for molecular systems of various sizes. The critical roles of orbital localization and describing the screening effect are understood by comparing results from lrLOSC and those from GSC2 and LOSC2. The localization procedure is essential for extended molecular systems, and the describing the screening effect improves the descriptions of all molecular systems. Additionally, in this paper, we explore the algebraic structure of lrLOSC, significantly enhancing its efficiency and achieving a computational cost comparable to that of the standard KS-DFT.

CONFLICT OF INTEREST

The authors have no conflicts to disclose.

ACKNOWLEDGMENTS

JY and WY acknowledge support from the National Institutes of Health (1R35GM158181).

AUTHOR CONTRIBUTIONS

Y.F. and J.Y. contributed equally to this paper.

DATA AVAILABILITY STATEMENT

The data that support the findings of this study are available within the article and its supplementary material.

REFERENCES

- P. Hohenberg and W. Kohn, "Inhomogeneous Electron Gas," *Phys. Rev.* **136**, B864–B871 (1964).
- W. Kohn and L. J. Sham, "Self-Consistent Equations Including Exchange and Correlation Effects," *Phys. Rev. A* **140**, 1133–1138 (1965).
- R. G. Parr and W. Yang, *Density-Functional Theory of Atoms and Molecules* (Oxford University Press, New York, 1989).
- S. H. Vosko, L. Wilk, M. Nusair, S. H. Vosko, L. Wilk, and M. Nusair, "Accurate spin-dependent electron liquid correlation energies for local spin density calculations: a critical analysis," *CaJPh* **59**, 1200 (1980).
- A. D. Becke, "Density-functional exchange-energy approximation with correct asymptotic behavior," *Phys. Rev. A* **38**, 3098–3100 (1988).
- C. Lee, W. Yang, and R. G. Parr, "Development of the Colle-Salvetti correlation-energy formula into a functional of the electron density," *Phys. Rev. B* **37**, 785–789 (1988).
- J. P. Perdew, K. Burke, and M. Ernzerhof, "Generalized Gradient Approximation Made Simple," *Phys. Rev. Lett.* **77**, 3865–3868 (1996).
- A. D. Becke, "A new inhomogeneity parameter in density-functional theory," *J Chem Phys* **109**, 2092–2098 (1998).
- J. Tao, J. P. Perdew, V. N. Staroverov, and G. E. Scuseria, "Climbing the Density Functional Ladder: Nonempirical Meta-Generalized Gradient Approximation Designed for Molecules and Solids," *Phys Rev Lett* **91**, 146401 (2003).
- R. Peverati and D. G. Truhlar, "M11-L: A local density functional that provides improved accuracy for electronic structure calculations in chemistry and physics," *J. Phys. Chem. Lett.* **3**, 117–124 (2012).
- J. Sun, R. C. Remsing, Y. Zhang, Z. Sun, A. Ruzsinszky, H. Peng, Z. Yang, A. Paul, U. Waghmare, X. Wu, M. L. Klein, and J. P. Perdew, "Accurate first-principles structures and energies of diversely bonded systems from an efficient density functional," *Nature Chem* **8**, 831–836 (2016).
- H. S. Yu, X. He, and D. G. Truhlar, "MN15-L: A New Local Exchange-Correlation Functional for Kohn-Sham Density Functional Theory with Broad Accuracy for Atoms, Molecules, and Solids," *J. Chem. Theory Comput.* **12**, 1280–1293 (2016).
- P. J. Stephens, F. J. Devlin, C. F. Chabalowski, and M. J. Frisch, "Ab Initio calculation of vibrational absorption and circular dichroism spectra using density functional force fields," *J. Phys. Chem.* **98**, 11623–11627 (1994).
- A. Savin and H.-J. Flad, "Density functionals for the Yukawa electron-electron interaction," *Int. J. of Quantum Chemistry* **56**, 327–332 (1995).
- T. Yanai, D. P. Tew, and N. C. Handy, "A new hybrid exchange–correlation functional using the Coulomb-attenuating method (CAM-B3LYP)," *Chem Phys Lett* **393**, 51–57 (2004).
- A. J. Cohen, P. Mori-Sánchez, and W. Yang, "Development of exchange–correlation functionals with minimal many-electron self-interaction error," *J Chem Phys* **126**, 191109 (2007).
- N. Mardirossian and M. Head-Gordon, "omega B97M-V: A combinatorially optimized, range-separated hybrid, meta-GGA density functional with VV10 nonlocal correlation," *J. Chem. Phys.* **144**, 214110 (2016).
- M. S. Hybertsen and S. G. Louie, "Electron correlation in semiconductors and insulators: Band gaps and quasiparticle energies," *Phys. Rev. B* **34**, 5390 (1986).
- I. Dabo, A. Ferretti, N. Poirvert, Y. Li, N. Marzari, and M. Cococcioni, "Koopmans' condition for density-functional theory," *Phys. Rev. B* **82**, 115121 (2010).
- T. Tsuneda, J. W. Song, S. Suzuki, and K. Hirao, "On Koopmans' theorem in density functional theory," *J. Chem. Phys.* **133**, 174101 (2010).
- L. Kronik, T. Stein, S. Refaelly-Abramson, and R. Baer, "Excitation gaps of finite-sized systems from optimally tuned range-separated hybrid functionals," *J. Chem. Theory Comput.* **8**, 1515–1531 (2012).
- J. Zheng, Y. Zhao, and D. G. Truhlar, "The DBH24/08 Database and Its Use to Assess Electronic Structure Model Chemistries for Chemical Reaction Barrier Heights," *J. Chem. Theory Comput.* **5**, 808–821 (2009).
- C. Li, X. Zheng, N. Q. Su, and W. Yang, "Localized orbital scaling correction for systematic elimination of delocalization error in density functional approximations," *Natl. Sci. Rev.* **5**, 203–215 (2018).
- Y. Mei, Z. Chen, and W. Yang, "Self-Consistent Calculation of the Localized Orbital Scaling Correction for Correct Electron Densities and Energy-Level Alignments in Density Functional Theory," *J. Phys. Chem. Lett.* **11**, 10269–10277 (2020).
- P. Mori-Sánchez, A. J. Cohen, and W. Yang, "Localization and delocalization errors in density functional theory and implications for band-gap prediction," *Phys. Rev. Lett.* **100**, 146401 (2008), arXiv: 0708.3688.
- A. J. Cohen, P. Mori-Sánchez, and W. Yang, "Insights into current limitations of density functional theory," *Science (80-)* **321**, 792–794 (2008).
- J. P. Perdew, R. G. Parr, M. Levy, and J. L. Balduz, "Density-Functional Theory for Fractional Particle Number: Derivative Discontinuities of the Energy," *Phys. Rev. Lett.* **49**, 1691–1694 (1982).
- W. Yang, Y. Zhang, and P. W. Ayers, "Degenerate ground states and a fractional number of electrons in density and reduced density matrix functional theory," *Phys. Rev. Lett.* **84**, 5172 (2000).
- T. Yanai, D. P. Tew, and N. C. Handy, "A new hybrid exchange–correlation functional using the Coulomb-attenuating method (CAM-B3LYP)," *Chem. Phys. Lett.* **393**, 51–57 (2004).
- G. Santra, R. Calinsky, and J. M. L. Martin, "Benefits of Range-Separated Hybrid and Double-Hybrid Functionals for a Large and Diverse Data Set of Reaction Energies and Barrier Heights," *J. Phys. Chem. A* **126**, 5492–5505 (2022).

³¹N. P. Brawand, M. Vörös, M. Govoni, and G. Galli, “Generalization of dielectric-Dependent hybrid functionals to finite systems,” *Phys. Rev. X* **6**, 41002 (2016).

³²J. P. Perdew and A. Zunger, “Self-interaction correction to density-functional approximations for many-electron systems,” *Phys. Rev. B* **23**, 5048–5079 (1981).

³³M. R. Pederson, A. Ruzsinszky, and J. P. Perdew, “Communication: Self-interaction correction with unitary invariance in density functional theory,” *J. Chem. Phys.* **140**, 121103 (2014).

³⁴V. I. Anisimov and A. V. Kozhevnikov, “Transition state method and Wannier functions,” *Phys. Rev. B* **72**, 75125 (2005).

³⁵H. J. Kulik, M. Cococcioni, D. A. Scherlis, and N. Marzari, “Density Functional Theory in Transition-Metal Chemistry: A Self-Consistent Hubbard U Approach,” *Phys. Rev. Lett.* **97**, 103001 (2006).

³⁶N. L. Nguyen, N. Colonna, A. Ferretti, and N. Marzari, “Koopmans-Compliant Spectral Functionals for Extended Systems,” *Phys. Rev. X* **8**, 021051 (2018).

³⁷N. Colonna, R. De Gennaro, E. Linscott, and N. Marzari, “Koopmans Spectral Functionals in Periodic Boundary Conditions,” *J. Chem. Theory Comput.* **18**, 5435–5448 (2022).

³⁸X. Zheng, A. J. Cohen, P. Mori-Sánchez, X. Hu, and W. Yang, “Improving band gap prediction in density functional theory from molecules to solids,” *Phys. Rev. Lett.* **107**, 026403 (2011).

³⁹C. Li, X. Zheng, A. J. Cohen, P. Mori-Sánchez, and W. Yang, “Local Scaling Correction for Reducing Delocalization Error in Density Functional Approximations,” *Phys. Rev. Lett.* **114**, 53001 (2015).

⁴⁰D. Zhang, X. Zheng, C. Li, and W. Yang, “Orbital relaxation effects on Kohn-Sham frontier orbital energies in density functional theory,” *J. Chem. Phys.* **142**, 154113 (2015).

⁴¹N. Q. Su, A. Mahler, and W. Yang, “Preserving Symmetry and Degeneracy in the Localized Orbital Scaling Correction Approach,” *J. Phys. Chem. Lett.* **11**, 1528–1535 (2020).

⁴²Y. Mei, Z. Chen, and W. Yang, “Exact second-order corrections and accurate quasiparticle energy calculations in density functional theory,” *J. Phys. Chem. Lett.* **12**, 7236–7244 (2021).

⁴³Y. Mei, J. Yu, Z. Chen, N. Q. Su, and W. Yang, “Libsc: Library for scaling correction methods in density functional theory,” *J. Chem. Theory Comput.* **18**, 840–850 (2022).

⁴⁴Y. Mei, C. Li, N. Q. Su, and W. Yang, “Approximating Quasiparticle and Excitation Energies from Ground State Generalized Kohn-Sham Calculations,” *J. Phys. Chem. A* **123**, 666–673 (2018).

⁴⁵X. Yang, X. Zheng, and W. Yang, “Density Functional Prediction of Quasiparticle, Excitation, and Resonance Energies of Molecules With a Global Scaling Correction Approach,” *Front. Chem.* **8**, 588808 (2020).

⁴⁶Y. Mei and W. Yang, “Charge transfer excitation energies from ground state density functional theory calculations,” *J. Chem. Phys.* **150**, 144109 (2019).

⁴⁷Y. Mei and W. Yang, “Excited-State Potential Energy Surfaces, Conical Intersections, and Analytical Gradients from Ground-State Density Functional Theory,” *J. Phys. Chem. Lett.* **10**, 2538–2545 (2019).

⁴⁸J. Li, Y. Jin, N. Q. Su, and W. Yang, “Combining localized orbital scaling correction and bethe-salpeter equation for accurate excitation energies,” *J. Chem. Phys.* **156**, 154101 (2022).

⁴⁹Y. Mei, N. Yang, and W. Yang, “Describing polymer polarizability with localized orbital scaling correction in density functional theory,” *J. Chem. Phys.* **154**, 054302 (2021).

⁵⁰J. Z. Williams and W. Yang, “Correcting Delocalization Error in Materials with Localized Orbitals and Linear-Response Screening,” (2024), arXiv:2406.07351 [cond-mat, physics:physics].

⁵¹J. Yu, Y. Mei, Z. Chen, Y. Fan, and W. Yang, “Accurate Prediction of Core-Level Binding Energies from Ground-State Density Functional Calculations: The Importance of Localization and Screening,” *J. Phys. Chem.* Lett. **16**, 2492–2500 (2025).

⁵²F. Gygi, J.-L. Fattebert, and E. Schwegler, “Computation of Maximally Localized Wannier Functions using a simultaneous diagonalization algorithm,” *Comput. Phys. Commun.* **155**, 1–6 (2003).

⁵³F. Giustino and A. Pasquarello, “Mixed Wannier-Bloch functions for electrons and phonons in periodic systems,” *Phys. Rev. Lett.* **96**, 216403 (2006).

⁵⁴R. Dawes and T. Carrington, Jr., “Using simultaneous diagonalization and trace minimization to make an efficient and simple multidimensional basis for solving the vibrational Schrödinger equation,” *J. Chem. Phys.* **124**, 054102 (2006).

⁵⁵A. Mahler, J. Z. Williams, N. Q. Su, and W. Yang, “Wannier functions dually localized in space and energy,” *Phys. Rev. B* **112**, 075137 (2025).

⁵⁶S. F. Boys, “Construction of Some Molecular Orbitals to Be Approximately Invariant for Changes from One Molecule to Another,” *Rev. Mod. Phys.* **32**, 296 (1960).

⁵⁷J. Yu, N. Q. Su, and W. Yang, “Describing chemical reactivity with frontier molecular orbitals,” *JACS Au* **2**, 1383–1394 (2022).

⁵⁸F. Long Gu, J. Yu, and W. Yang, “Chemical concepts from molecular orbital theory,” Exploring Chemical Concepts Through Theory and Computation, 1–22 (2024).

⁵⁹A. Mahler, J. Williams, N. Q. Su, and W. Yang, “Localized orbital scaling correction for periodic systems,” *Phys. Rev. B* **106**, 035147 (2022).

⁶⁰W. Yang, A. J. Cohen, F. De Proft, and P. Geerlings, “Analytical evaluation of Fukui functions and real-space linear response function,” *J. Chem. Phys.* **136**, 144110 (2012).

⁶¹O. Vähtä, J. Almlöf, and M. W. Feyereisen, “Integral approximations for LCAO-SCF calculations,” *Chem. Phys. Lett.* **213**, 514–518 (1993).

⁶²X. Ren, P. Rinke, V. Blum, J. Wieferink, A. Tkatchenko, A. Sanfilippo, K. Reuter, and M. Scheffler, “Resolution-of-identity approach to Hartree-Fock, hybrid density functionals, RPA, MP2 and GW with numeric atom-centered orbital basis functions,” *New J. Phys.* **14**, 053020 (2012), arXiv: 1201.0655.

⁶³William H. Press, Brian P.P. Flannery, Saul A. Teukolsky, and William T. Vetterling, “Sparse Linear-Systems,” in *Numerical Recipes in C: The Art of Scientific Computing* (Cambridge University Press, New York, 1988) pp. 72–81.

⁶⁴A. J. Cohen, P. Mori-Sánchez, and W. Yang, “Fractional charge perspective on the band gap in density-functional theory,” *Phys. Rev. B - Condens. Matter Mater. Phys.* **77**, 115123 (2008).

⁶⁵W. Yang, A. J. Cohen, and P. Mori-Sánchez, “Derivative discontinuity, bandgap and lowest unoccupied molecular orbital in density functional theory,” *J. Chem. Phys.* **136**, 204111 (2012).

⁶⁶A. R. M. Shahi, C. J. Cramer, and L. Gagliardi, “Second-order perturbation theory with complete and restricted active space reference functions applied to oligomeric unsaturated hydrocarbons,” *Phys. Chem. Chem. Phys.* **11**, 10964–10972 (2009).

⁶⁷R. M. Richard, M. S. Marshall, O. Dolgounitcheva, J. V. Ortiz, J. L. Brédas, N. Marom, and C. D. Sherrill, “Accurate Ionization Potentials and Electron Affinities of Acceptor Molecules I. Reference Data at the CCSD(T) Complete Basis Set Limit,” *J. Chem. Theory Comput.* **12**, 595–604 (2016).

⁶⁸L. A. Curtiss, K. Raghavachari, P. C. Redfern, and J. A. Pople, “Assessment of Gaussian-2 and density functional theories for the computation of enthalpies of formation,” *J. Chem. Phys.* **106**, 1063–1079 (1997).

⁶⁹D. Hait and M. Head-Gordon, “Delocalization Errors in Density Functional Theory Are Essentially Quadratic in Fractional Occupation Number,” *J. Phys. Chem. Lett.* **9**, 6280–6288 (2018).

⁷⁰C. Li and W. Yang, “On the piecewise convex or concave nature of ground state energy as a function of fractional number of electrons for approximate density functionals,” *J. Chem. Phys.* **146**, 074107 (2017).

⁷¹T. H. Dunning, “Gaussian basis sets for use in correlated molecular calculations. I. The atoms boron through neon and hydrogen,” *J. Chem. Phys.* **90**, 1007–1023 (1989).